Mechanism of generating fast electrons by an intense laser at a steep overdense interface

J. May, J. Tonge, F. Fiuza, R. A. Fonseca, L. O. Silva, C. Ren, and W. B. Mori

Phys. Rev. E **84**, 025401 — Published 3 August 2011

DOI: 10.1103/PhysRevE.84.025401

On the mechanism of generating fast electrons by an intense laser at a steep overdense interface

J. May[(a)], J. Tonge[(a)], F. Fiuza[(c)], R. A. Fonseca[(c)], L.O. Silva[(c)], C. Ren[(d)], and W.B. Mori[(a,b)]
[(a)] *Department of Physics and Astronomy, University of California, Los Angeles, Los Angeles, California 90095*
[(b)] *Department of Electrical Engineering, University of California, Los Angeles, Los Angeles, California 90095*
[(c)] *GoLP/Instituto de Plasmas e Fusão Nuclear - Laboratório Associado, Instituto Superior Tecnico, 1049-001 Lisboa, Portugal and*
[(d)] *Department of Mechanical Engineering, University of Rochester*

The acceleration and heating of electrons by an intense laser normally incident on a steep overdense plasma interface is investigated using the particle-in-cell code OSIRIS. Energetic electrons are generated by the laser's electric field in the vacuum region within $\lambda/4$ of the surface. Only those electrons which originate within the plasma with a sufficiently large transverse momentum can escape the plasma. This mechanism relies on the standing wave structure created by the incoming and reflected wave and is therefore very different for linear and circularly polarized light.

PACS numbers: 52.57.Kk, 52.50.Jm, 52.38.Dx, 52.65.Rr

Understanding the collisionless absorption of an intense laser via the generation of energetic electrons at a steep overdense plasma interface is fundamental to the development of fast ignition fusion [1–3] and laser driven ion acceleration from solids [4–6]. It is also a fundamental topic in nonlinear wave particle interactions.

A laser is absorbed at a steep overdense plasma interface by mechanisms different than resonance absorption because there is no clear location for a resonance. The two most commonly invoked absorption mechanisms for steep interfaces are $J \times B$ heating [7] and Brunel absorption [8]. In the original work of Kruer and Estabrook [7], $J \times B$ heating referred to the heating by a longitudinal electric field generated within a skin depth inside the plasma at the second harmonic of the laser by the $v \times B$ force. In the years since this original work, the mechanism has been invoked whenever the electron bunches stream inwards at the second harmonic of the laser without considerating if the acceleration is occurring just inside or outside the plasma. This process can occur for lasers incident at normal incidence. Conversely, the Brunel mechanism [8] (originally called "not so resonant, resonant absorption") results from the anharmonic motion of an electron by the normal component of the laser's field when it is incident at an oblique angle in the plane of the density gradient (P polarization).

Very recently, Kemp *et al.* [9] have used one-dimensional particle-in-cell simulations to study hot-electron generation by an intense laser at a steep interface at normal incidence. They explained their results in terms of the standing wave generated by the incoming laser and a reflected wave, together with a longitudinal (normal) electric field at the surface which pulls electrons out of the plasma. Their analysis indicates that the maximum energy scales as $1.45 a_0 mc^2$ where $a_0 = eA/mc^2$ is the normalized vector potential of the laser. Specifically, they predict no heating or absorption without a low density shelf and the corresponding longitudinal E-field.

In this letter, we propose a different heating and acceleration process that can occur for normal incidence. Using the particle-in-cell code OSIRIS [10], we show that the energetic electrons are accelerated by the laser's electric field in the vacuum region within a quarter wavelength of the surface. The simulations show that this mechanism relies strongly on the standing wave structure created by the incoming and reflected wave; in particular, the surface B-field of the standing wave plays a crucial role, as it prevents electrons from penetrating into the vacuum unless they leave at a phase when it is decreasing in magnitude. At such a phase thermal (or otherwise heated) electrons can be rotated as they leave the plasma, transverse momentum being converted into normal motion, allowing them to penetrate the vacuum region a distance sufficient to reach the peak E-field. With linear polarization electrons in phase with the standing wave gain a maximum momentum of $2a_0 mc^2$. However, for circularly polarized light the B-field strength never decreases at the surface, preventing electrons from ever reaching the high field region and there accelerating.

This mechanism cannot be equated with the $J \times B$ mechanism as energy is gained in the vacuum from the transverse laser field, and it is distinct from Brunel heating as it occurs for normal incidence. Furthermore, it sheds light on the ponderomotive scaling found by Wilks *et al.* [11] and the recent observation that ion acceleration, which depends on the heated electron temperature, is dramatically different between linear and circular polarized light [5, 12]. Our mechanism differs significantly from Kemp *et al.* [9]. Most importantly, we find that only electrons which originate inside the plasma with a large transverse momentum can penetrate into the vacuum, because of the importance of the surface B-field which rotates the electrons so their motion is normal to the surface as they move into vacuum. No surface normal electric field nor low density shelf is required. In addition, one-dimensional "cold" plasmas give no absorption.

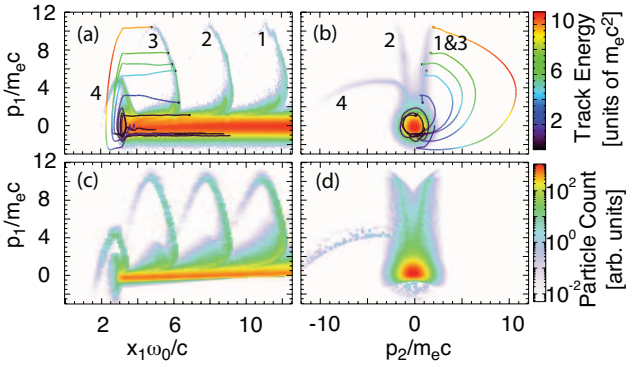

FIG. 1: (Color) Top row: electron phasespaces, (a) p_1 vs. x_1 and (b) p_1 vs. p_2, for an OSIRIS simulation with $a_0 = 6$ at $t = 13.85\omega_0^{-1}$, with tracks for individual particles superimposed. Bunches of electrons are labeled 1-4. Bottom row: Same phasespace plots for test particles moving in a standing wave with $a_0 = 6$.

To illustrate the physics, we use OSIRIS [10], in either a $1\frac{2}{2}D$ or $2\frac{1}{2}D$ PIC geometry. We use planar targets with the plasma density rising rapidly from vacuum to a density of $100n_c$. The incident laser (plane wave) also rises rapidly to a peak intensity after which it is held constant. It is launched in the x_1 (or z) direction into a vacuum region, of $\lambda/2$ for fixed ion runs, or up to 24λ for mobile ion runs, where λ is the wavelength of the laser. The plasma fills the box in the transverse x_2 (or x) direction, where we use periodic boundary conditions for both the particles and the fields. In the x_1 direction we have absorbing boundaries for the fields and thermalizing boundaries for the particles. We use cubic splines for the particle shape and current smoothing with compensation.

We begin by presenting results from a 2D simulation with immobile ions. The plasma electrons are initialized with a maxwellian distribution, $e^{-(u/2u_{th})^2}$, where u is the proper velocity and $u_{th} = 0.548$ in each direction (this corresponds to a temperature of $75keV$.) The incident laser has an a_0 of 6, which roughly corresponds to an intensity of $5 \cdot 10^{19} W/cm^2$ for a $1\mu m$ laser. The simulation box size was 4 λ long and 1.6 λ wide, with 630 cells per λ in each direction, which corresponds to 10 cells per skin depth (c/ω_p); 16 particles per cell were used.

As the laser pulse interacts with the plasma it accelerates electrons in bunches ('arms', labeled 1-4, in the p_1 vs. x_1 phasespace of Fig. 1a) which are spaced $\lambda/2$ apart. The higher energy particles are at the back of each bunch, causing the arms to curve back towards the surface. This is because, as seen in the particle tracks ending on arm 3, the higher momentum particles make correspondingly larger excursions into the vacuum, thereby re-entering the plasma later in time. The shape then remains because all electrons are traveling relativistically.

Looking at the tracks in Fig. 1b, it can be seen that the acceleration phase consists of electrons gaining momentum in p_2, then being rotated into the forward direction, with little change in energy during this rotation. We indicate how alternate bunches in 1a coincide with the same 'legs' in 1b.

It is important to note that all of the accelerated electrons are displaced from the $p_2 = 0$ axis, i.e., have non-vanishing p_2. Translational invariance in the x_2 direction implies that translational canonical momentum is strictly conserved. Since all of the plasma electrons originate inside the plasma where the laser field (vector potential) is zero – so that canonical and physical momentum are equivalent – any transverse momentum carried by the particles into the plasma must have also been carried out with them. Therefore, the fact that there are no accelerated particles on axis in Fig. 1b, means that it is necessary for particles to exit the plasma at an angle to the surface for acceleration to occur.

To understand the acceleration and heating mechanism, we next examine the equations of motion in prescribed fields together with the trajectories of individual electrons taken from simulations. We consider plane waves propagating along $\hat{z}(\hat{x}_1)$ with the $\vec{E}$ field polarized along $\hat{x}(\hat{x}_2)$ for which the equations of motion are $\frac{d}{dt}P_z = -e\frac{v_x}{c}B_y$ and $\frac{d}{dt}P_x = -e(E_x + \frac{v_z}{c}B_y)$. For simplicity we assume 100% reflection and that the plasma acts like a perfect conductor, for which $\frac{e\vec{A}}{m_e c^2} = [a_0 sin(kz - \omega t) + a_0 sin(kz + \omega t)]\hat{x} = 2a_0 sin(kz)cos(\omega t)\hat{x}$, $\frac{e\vec{E}}{m_e c\omega} = 2a_0 sin(kz)sin(\omega t)\hat{x}$, and $\frac{e\vec{B}}{m_e c\omega} = 2a_0 cos(kz)cos(\omega t)\hat{y}$ for $z < 0$ (and all vanish for $z > 0$.) Because $\vec{A}$ is only a function of z it follows from the equations of motion in the $\hat{x}$ direction that transverse canonical momentum is conserved, giving $\frac{P_x(t)}{m_e c} = \frac{P_x(t=0)}{m_e c} + 2a_0 sin(kz)cos(\omega t)$ for $z < 0$, and $\frac{P_x(t)}{m_e c} = \frac{P_x(t=0)}{m_e c}$ for $z > 0$.

The E_y field has a node at $z = 0$ and an anti-node at $z = -\frac{\lambda}{4}$, while B_x has an anti-node at $z = 0$. In the vacuum region the energy gain can only come from E_y, so the electron must penetrate nearly $\frac{\lambda}{4}$ into the vacuum in order to gain significant energy. However if the electron leaves when $|\vec{B}|$ is a maximum ($e\vec{B}_{max}/m_e c\omega = 2a_0$), then the Larmor radius ($\omega_0 r_L/c = u/2a_0$) will be small compared to $\lambda/4$ for high intensity lasers ($a_0 >> 1$). Thus the surface B field prevents significant acceleration (heating) of the electrons. On the other hand if an electron leaves at a phase where the $|B|$ field is smaller and decreasing then the surface B field can deflect the electron so it moves normal to the surface. If the velocity is near the speed of light then in a quarter period the electron can move near a quarter wavelength where $|E|$ is now approaching a maximum (if $|B|$ was increasing then $|E|$ would be decreasing as the electron entered the vacuum). The E_x field then rapidly accelerates the electron in the $\hat{x}$ direction to $\frac{P_x}{mc} \cong \frac{P_{x0}}{mc} \pm 2a_0$ (depending on the

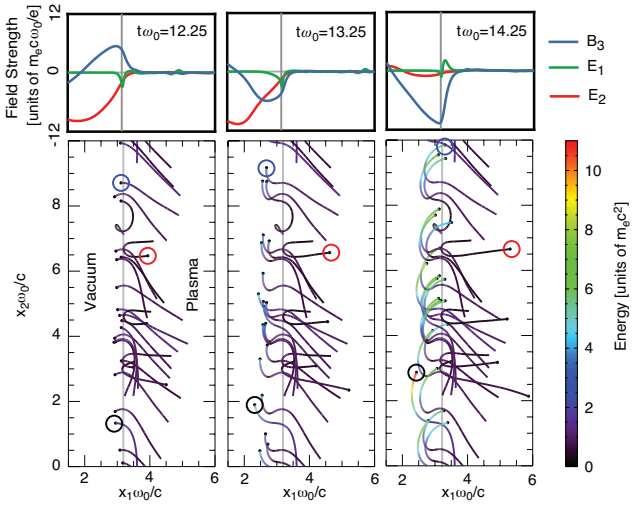

FIG. 2: (Color) Top row : Electric and magnetic fields near the surfac for $t = 12.25\omega_0^{-1}$, $13.25\omega_0^{-1}$, and $14.25\omega_0^{-1}$. Bottom row: Electron tracks (colored by energy) for the same simulation times. Key tracks are identified by circles.

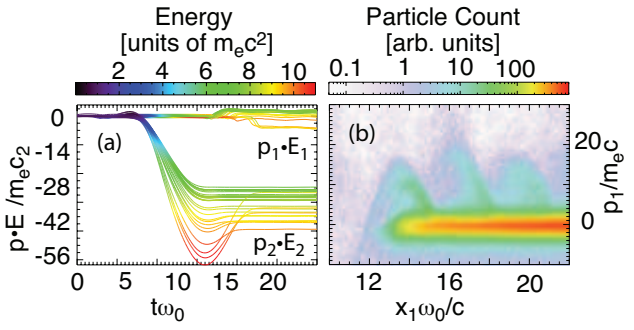

FIG. 3: (Color) (a)Time history of $\vec{p} \cdot \vec{E}$ for accelerated electrons for $a_0 = 6$, showing E_2 is the source of energy gain. (b)p_1 vs. x_1 phasespace after 500fs with mobile ions for $a_0 = 12$ shows the $2a_0$ signature remains.

sign of the $\vec{E}$ field), at which time the magnetic field of the forward moving wave bends the particle trajectory converting P_x into P_z. The electron reenters the plasma with a $P_z \lesssim 2a_0$.

This is clearly illustrated in Fig. 1 and in the particle tracks shown in Fig. 2. Figures 1c,d show the phasespace of test electrons (initialized with a maxwellian distribution with $u_{th} = 0.6$) in the electric and magnetic fields of a pure standing wave structure (reflection from a perfect conductor). The similarities between the test particle and self-consistent OSIRIS simulation is striking and confirms that the acceleration and heating process is due to the laser's electric field in vacuum and from the standing wave structure.

Fig. 2 shows the electron trajectories and the E_1, E_2, and B_3 fields at different times within a half laser period. Electrons which move normal to the surface inside the plasma, like the one indicated by a red circle, never escape because the surface B field reflects them. Electrons moving upwards (those with positive P_{x0}, one circled in blue) inside the plasma get deflected by B_3, which is decreasing at $\omega_0 t = 12.25$. They leave normal to the surface and then E_2 rapidly accelerates them upward (E_2 is negative). They are then rotated forward by B_3. The track which gains the most energy (black circle) was moving nearly parallel to, and within a skin depth of, the surface before B_3 deflected it. A half laser period later the same process can occur, except the electrons which are deflected out are moving down and the sign of the fields are reversed. Each leg in Fig. 1b corresponds to electrons initially moving up or down, respectively.

The distance the electrons penetrate into the vacuum is less than $\lambda/4$. However, from the fields shown in Fig. 2 it is clear that the standing wave is distorted, because the plasma is not a perfect conductor (fields exist in the plasma within a skin depth of the surface) and $|E_2|$ is a maximum at 0.21λ not 0.25λ from the surface.

It can be seen in Fig. 2 that E_z is very small and exists in a very narrow region so that it plays a negligible role in the acceleration process. To quantify this we track the components of $\vec{p} \cdot \vec{E} = \frac{d}{dt}\gamma^2$ for several electrons. The results are shown in Fig. 3a. It can be clearly seen that all of the energy gained is directly transferred from the laser field, and not through the surface space charge field. In fact the phase of E_z is such that at the point in time where the electrons leave the plasma it is pulling them back into the plasma, rather than pulling them out into the vacuum.

Based on the physical picture for the $2a_0$ acceleration mechanism, several important points are worth discussing. One is that it will be absent for cold plasmas. Electrons need an initial transverse momentum approaching mc to penetrate a large fraction of $\lambda/4$ into the vacuum region. In a 1D or 2D s-polarized simulation where the transverse canonical momentum is strictly conserved it is not possible for the transverse momentum inside the plasma to change (since A nearly vanishes inside the plasma). Therefore initially cold 1D like plasmas will not heat much; we have confirmed this in simulations. However, efficient $2a_0$ heating can occur for low initial temperatures for p-polarized light in multi-dimensions, where the surface can ripple and/or the laser filaments. For such cases there is a component of the laser electric field normal to the surface and effects such as Brunel heating can occur. Viewed another way, when the surface ripples translational invariance is broken in the laser polarization direction so the transverse momentum near the plasma surface can rapidly increase. After the plasma surface heats from these other mechanisms, the $2a_0$ process can be accessed. To illustrate this we present results from a 2D simulation with a p-polarized laser and mobile ions with $a_0 = 12$. The plasma is initialized with a temperature of 1 keV, the transverse dimension is 3 λ with

63 cells/λ in each direction. We use 16 particles per cell for both the electrons and the ions.

The p_1 vs. x_1 phasespace, at time $t = 500$fs for $\lambda = 1\mu$, is shown in Fig. 3b. Initially the reflectivity is very high, and there are no particles accelerated to the MeV range. The plasma quickly develops a hot surface layer of roughly 50keV after 50fs in this simulation. Once formed, this layer supplies a store of electrons with enough kinetic energy to traverse the reflecting magnetic field and reach the accelerating field, initially having phasespace plots much like that shown in Fig. 1a. Later in times at 500fs (although not as well defined) the shape and spacing of the bunches in Fig. 3b is still consistent with the $2a_0$ mechanism. Reasons for blurring of the bunches are that late in time absorption increases and the plasma surface becomes greatly perturbed, significantly modifying the standing wave pattern.

We have also studied how this process scales with a_0, and how the resulting energy spectra relates to ponderomotive scaling. In Fig. 4a we plot a series of spectra from 2D simulations, where a_0 was varied from 3 to 24, and an initially cold plasma (1keV) was allowed to heat self-consistently. Each spectrum is measured in the first $3/2\lambda$ inside the plasma, early in time before a plasma shelf forms. For reference two 1D runs are also shown, with $T_e = 0.6keV$ and $T_e = 125keV$, showing that the "cold" plasma has no accelerated electrons. (Temperatures between these two extremes show electrons accelerated to energies roughly proportional to the temperature; the first $2a_0$ electrons appear at about 60keV for these parameters.) The p_1 values have been normalized to $2a_0m_ec$, clearly showing the self-similarity of the interaction, and the sharp cutoff in maximum energy. We find this distribution gradually relaxes as the electrons traverse the plasma due to coherent wakefields generated by the electron bunches.

In Fig. 4b we show the spectra for a simulation of Fig. 3b at 50fs near the surface and at 500fs throughout the plasma. The early time surface spectra is relatively flat and cuts off at $2a_0m_ec$. However late in time two temperatures of forward accelerated electrons can be seen, one with half the ponderomotive scaling and extending to $2a_om_ec$, and one with the full ponderomotive scaling above that. The lower energy electrons can be associated with the $2a_0$ mechanism. The hottest electrons are those generated in an underdense shelf, where plasma electrons can interact many times with the incoming and reflected laser, stochastically gaining energy. This was also described previously by Kemp [9]. However these particles carry very little of the net energy. This trend has been observed in larger scale fast ignition simulations [13].

The $2a_0$ process is basically absent for circularly polarized lasers. The magnetic field in the standing wave at the plasma surface never decreases to zero, rather it rotates with a constant magnitude. As a result an electron can only penetrate a distance roughly equal to the Larmor radius for the peak B field. We carried out an identical simulation to that for Fig. 1a except the laser was circularly polarized and we saw no electron accelerated above the thermal plasma. This may be the dominant reason why the proton acceleration is so different for circularly polarized light (called RPA [5]), since proton acceleration driven by high mach number shocks requires relativistic electron temperatures [6].

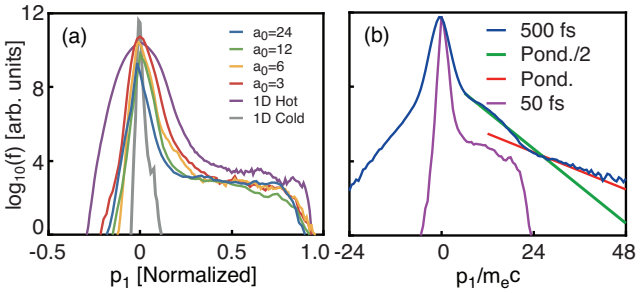

FIG. 4: (Color) (a) Surface spectra at early times for six simulations. Initial $T_e = 1keV$ except for the 1D cases. (b) Early (50fs) and late (500fs) spectra for $a_0 = 12$. Late spectrum shows two hot electron temperatures with break at $\sim 2a_0m_ec$.

In summary, we have presented a new mechanism for electron acceleration by ultrahigh intensity lasers interacting with highly overdense plasmas at normal incidence. The main features of this mechanism have been studied using simulations and theory, including particle tracking, showing that it can play an important role in typical fast ignition and laser-driven ion acceleration configurations, and shedding light on the origin of the different components of the electron spectrum observed in these scenarios.

We acknowledge useful conversations with Prof. C. Joshi. Work supported by The DOE Fusion Science Center for Matter Under Extreme Conditions and DOE contract DE-FG03-09NA22569, by NSF grant Phy-0904039 and Phy-0936266, by FCT (Portugal) through the grants PTDC/FIS/66823/2006 and SFRH/BD/38952/2007, and by the European Community (HiPER project EC FP7 no. 211737). The simulations were performed on the Hoffman2 cluster at UCLA.

[1] M. Tabak *et al.*, Phys. Plasmas **1**, 1626 (1994).
[2] S. Atzeni, Phys. Plasmas **6**, 3316 (1999).
[3] R. Kodama *et al.*, Nature **412**, 798 (2001).
[4] B. M. Hegelich *et al.*, Nature **439**, 441 (2006).
[5] A. P. L. Robinson *et al.*, New J. Phys. **10**, 013021 (2008).
[6] L. O. Silva *et al.*, Phys. Rev. Lett. **92**, 015002 (2004).
[7] W. L. Kruer and K. Estabrook, Phys. Fluids **28**, 430 (1985).
[8] F. Brunel, Phys. Rev. Lett. **59**, 52 (1987).
[9] A.J. Kemp, Y. Sentoku, and M. Tabak, Phys. Rev. E **79**, 066406 (2009).

[10] R. A. Fonseca *et al.*, Lect. Notes Comp. Sci. **2331**, 342 (2002).
[11] S.C. Wilks, W.L. Kruer,M. Tabak, and A.B. Langdon, Phys. Rev. Lett. **69**,1383 (1992).
[12] B. Qiao *et al.*, Phys. Rev. Lett. **105**, 155002 (2010).
[13] J. Tonge *et al.*, Phys. Plasmas **16**, 056311 (2009).